The Astrophysical Journal, 630:1206–1212, 2005 September 10


# EVOLUTION OF SOLAR SUBSURFACE MERIDIONAL FLOWS IN THE DECLINING PHASE OF CYCLE 23

Dean-Yi Chou and Oleg Ladenkov
Institute of Astronomy and Department of Physics, National Tsing Hua University, Hsinchu 30043, Taiwan; chou@phys.nthu.edu.tw
*Received 2005 March 9; accepted 2005 May 26*

## ABSTRACT

We study the evolution of meridional flows in the solar convection zone extending to a depth of 0.793 $R_\odot$ in the period 2000–2003 with helioseismic data taken with the Taiwan Oscillation Network (TON) using the technique of time-distance helioseismology. The meridional flows of each hemisphere formed a single-cell pattern in the convection zone at the solar minimum. An additional divergent flow was created at active latitudes in both hemispheres as the activity developed. The amplitude of this divergent flow correlates with the sunspot number: it increased from solar minimum to maximum (from 1996 to 2000), and then decreased from 2000 to 2003 with the sunspot number. The amplitude of the divergent flow increases with depth from 0.987 $R_\odot$ to a depth of about 0.9 $R_\odot$, and then decreases with depth at least down to 0.793 $R_\odot$.

*Subject headings:* Sun: activity — Sun: helioseismology — Sun: interior — sunspots

## 1. INTRODUCTION

The meridional flows play an important role in understanding the differential rotation and energy transport in the solar convection zone. They have been extensively studied for over two decades. The surface meridional flows have been measured by using tracers on the surface (Howard & Gilman 1986; Komm et al. 1993; Snodgrass & Dailey 1996; Nesme-Ribes et al. 1997; Meunier 1999) or by directly measuring the surface Doppler shifts (Duvall 1979; LaBonte & Howard 1982; Hathaway et al. 1996). The meridional flows are poleward in both hemispheres, with an amplitude of 10–20 m $s^{-1}$.

The first evidence of subsurface meridional flow was obtained by measuring the difference between northward and southward acoustic wave travel times with the technique of time-distance helioseismology (Giles et al. 1997). Its follow-up measurements show that the meridional flow extends through the entire solar convection zone (0.71–1.0 $R_\odot$; Giles 1999). Inversion of measured travel-time difference infers that the meridional flow in the convection zone has a single-cell pattern if the mass conservation is imposed (Giles 1999). Material in the upper convection zone moves poleward from the equator to about 60° latitude with a peak velocity of 20 m $s^{-1}$, and returns equatorward in the lower convection zone.

Measurements using frequency shifts have also shown evidence of subsurface meridional flow down to ~0.86 $R_\odot$ (Braun & Fan 1998). Measurements with ring diagrams have shown that meridional flow exists in the region from the surface to 0.97 $R_\odot$ (Gonzalez Hernandez et al. 1999; Basu & Antia 2000).

Chou & Dai (2001, hereafter Paper I) have applied the technique of time-distance helioseismology to the helioseismic data taken with the Taiwan Oscillation Network (TON) to study solar cycle variations of meridional flows in the range 0.9–0.987 $R_\odot$ from 1994 to 2000, covering the solar minimum in 1996 and the maximum in 2000. They discovered that a new component of meridional flow, centered at about 20° latitude, was created in both hemispheres as the surface magnetic activity developed during 1998–2000. The new component is a divergent flow: it moves northward and southward away from its center. The additional divergent flow changes the observed meridional flow from poleward at solar minimum to equatorward at solar maximum at low latitudes. The center of the divergent component of meridional flow approximately coincides with the center of sunspot distribution and migrates from ~25° latitude in 1998 to ~15° in 2000. This finding has been confirmed by Beck et al. (2002). They have also shown that variations of this divergent meridional flow correlate with variations of torsional oscillations and magnetic flux. Haber et al. (2002) used the ring diagram technique to study the evolution of meridional flows in the period 1998–2001 in the outer 10 Mm (~0.014 $R_\odot$). They found the appearance of an additional cell in the northern hemisphere in this period.

Paper I showed that the amplitude of the additional divergent flow increased with surface magnetic activity from 1997 to 2000. The amplitude also increased with depth at least down to 0.9 $R_\odot$. In Paper I, three questions were raised. First, how will the additional divergent flow evolve as the surface activity decreases after solar maximum? Second, how deep does the additional divergent flow penetrate into the convection zone? Third, what is the origin of the additional divergent flow? Here we provide information on the first two questions.

In this study, we use TON data to study the evolution of the additional divergent meridional flow in the declining phase of Cycle 23 (from 2000 to 2003). We improve the data analysis to obtain a higher signal-to-noise ratio for large travel distances. This allows us to extend the range of study to 0.793–0.987 $R_\odot$, about two-thirds of the convection zone. We find that the amplitude of the divergent flow decreased as the surface magnetic activity decreases from 2000 to 2003. The amplitude of the divergent flow increases with depth from 0.987 $R_\odot$ and reaches the maximum value at about 0.9 $R_\odot$. Then it decreases with depth at least down to 0.793 $R_\odot$. In § 2 we describe the data and analysis, in § 3 we discuss evolution of meridional flows, and in § 4 we discuss depth variations of meridional flows.

## 2. DATA AND ANALYSIS

In this study, we use the helioseismic data taken with TON. The TON data are full-disk K-line imaged, recorded by a 16-bit $1080 \times 1080$ CCD. The images are taken at a rate of one image per minute. The diameter of the Sun is about 1000 pixels. The measured amplitude of intensity oscillation is about 2.5%. A discussion of the TON project and its instruments is given by Chou et al. (1995). The preliminary data reduction of the TON data, such as flat fielding, registration, and limb-darkening correction,

is given by Chen et al. (1996). Six years of data are used in this study, including the minimum period 1996–1997 and the declining phase of Cycle 23, 2000–2003. Here we use the data taken with the TON telescope at the Big Bear Solar Observatory. The time series taken on each day is analyzed separately; a total of 663 time series are analyzed. The data reduction is similar to that in Paper I, but with some improvement in order to increase the signal-to-noise ratio, especially for the larger angular distances, corresponding to the deeper regions.

In Paper I, the signal-to-noise ratio (S/N) for the travel distance greater than 16° is too low to provide useful information on the meridional flows deeper than 0.9 $R_\odot$. One of the sources of noise is the large-scale nonuniformity in the data. In this study, we reduce the large-scale nonuniformity in each image by subtracting the $41 \times 41$ pixel spatial running mean. This improvement is demonstrated by the fact that the artifact in the cross-correlation function is reduced.

Here we briefly describe the data reduction procedure.

1. Each observed K-line full-disk image is transformed into coordinates of $\sin\theta$ and $\phi$, where $\theta$ and $\phi$ are the latitude and longitude, respectively, in a spherical coordinate system aligned along the solar rotation axis.

2. The oscillatory amplitude is computed by subtracting the 15-frame running mean from the intensity time series at each spatial point.

3. The data are filtered with a Gaussian filter of FWHM = 1.3 mHz (1 mHz in Paper I) centered at 3.5 mHz.

4. For each image, the $41 \times 41$ pixel spatial running mean is subtracted from the signal at each point.

5. The cross-correlation function between two points at the same longitude is computed with

$$C(\theta,\ \phi,\ \Delta,\ \tau) = \int \Psi\left(\theta - \frac{\Delta}{2},\ \phi,\ t\right)\Psi\left(\theta + \frac{\Delta}{2},\ \phi,\ t+\tau\right)dt, \quad (1)$$

where $(\theta - \Delta/2,\ \phi)$ and $(\theta + \Delta/2,\ \phi)$ are the coordinates of two points, $\Delta$ is the angular distance between two points, and $\tau$ is the time shift.

6. The computation of the cross-correlation function is repeated for different $\theta$, $\phi$, $\Delta$, and $\tau$. The step of $\sin\theta$ is 1/512. The range of $\theta$ is $(-65°,\ 65°)$ for $\Delta \le 21°$, and $(-45°,\ 45°)$ for $\Delta > 21°$. The step of $\phi$ is 0.°176 in a range of $-60° < \phi < 60°$. The step of $\tau$ is 1 minute. The step of $\Delta$ is 0.°2. The range of $\Delta$ is 1°–32°.

7. The cross-correlation functions $C(\theta, \phi, \Delta, \tau)$ are averaged to increase the S/N. First, $C(\theta, \phi, \Delta, \tau)$ are averaged over longitude $\phi$ to become $C(\theta, \Delta, \tau)$. Second, $C(\theta, \Delta, \tau)$ are binned every 5° in latitude $\theta$.

8. The above procedure is repeated for different time series. The cross-correlation functions $C(\theta, \Delta, \tau)$ are averaged over a year to increase the S/N.

9. The phase travel time is determined from the instantaneous phase of the yearly averaged cross-correlation function with a Hilbert transform technique (Bracewell 1986). The procedure is carried out for both positive and negative $\tau$ to obtain northward and southward travel times, respectively.

10. The difference between the northward and southward travel times, $\delta\tau(\theta, \Delta)$, is caused by the longitude-averaged meridional flow along the ray path centered at latitude $\theta$ (Giles et al. 1997; Giles 1999). The sign is chosen such that the positive $\delta\tau$ corresponds to northward motion, and the negative corresponds to southward motion.

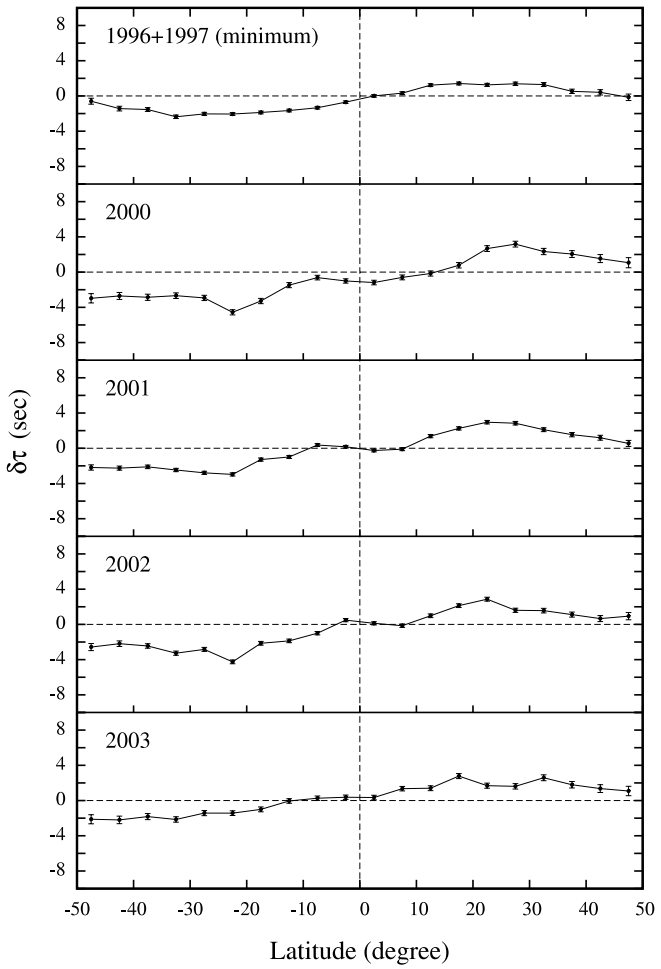


FIG. 1.—Time difference $\delta\tau$ vs. latitude for different years, showing the average over angular distance 2°–6°, corresponding to the range of depth 0.987–0.962 $R_\odot$. The positive $\delta\tau$ corresponds to northward motion, and the negative corresponds to southward motion.

Different travel distances $\Delta$ correspond to different ray paths. The larger the travel distance, the deeper the ray path is. Hence, the time difference $\delta\tau(\theta, \Delta)$ carries information on the velocity distribution of subsurface meridional flow in the convection zone. To obtain the velocity distribution of subsurface meridional flow as a function of latitude and depth, one needs to invert $\delta\tau(\theta, \Delta)$. However, the forward and inversion study (Giles et al. 1998; Giles 1999) has shown that $\delta\tau$ is approximately linearly proportional to the flow speed in the mode cavity; a time difference of 1 s corresponds to a flow speed of about 10 m s$^{-1}$ in the range of $\Delta$ studied here. In this study, we do not carry out the inversion; instead, we use $\delta\tau(\theta, \Delta)$ to show solar cycle variations of meridional flows in the solar convection zone.

To increase the S/N, $\delta\tau(\theta, \Delta)$ is averaged over angular distance $\Delta$ for five different ranges: $\Delta = 2°$–6° (corresponding to the lower turning point in the range of 0.987–0.962 $R_\odot$), 6°–10° (0.962–0.938 $R_\odot$), 10°–16° (0.938–0.901 $R_\odot$), 16°–22° (0.901–0.864 $R_\odot$), and 22°–32° (0.864–0.793 $R_\odot$).

## 3. SOLAR CYCLE VARIATIONS OF MERIDIONAL FLOWS

Paper I showed that the amplitude of the additional divergent flow increased from solar minimum (1996–1997) to maximum (2000). Here we investigate temporal variations of meridional flows in the declining phase of Cycle 23, from 2000 to 2003. The

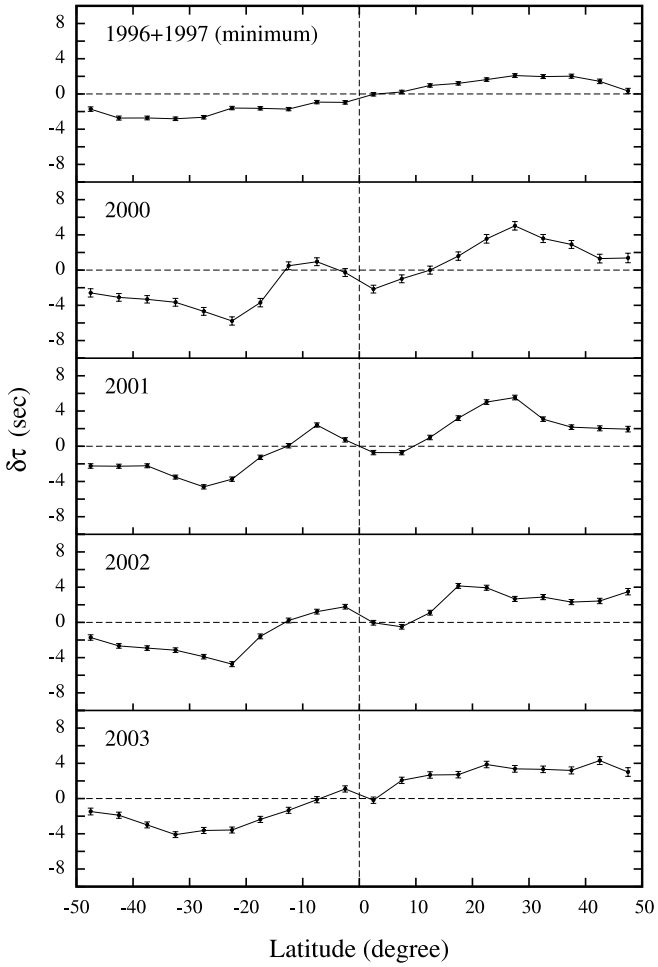


FIG. 2.—Time difference $\delta\tau$ vs. latitude for different years, showing the average over angular distance $6^\circ$–$10^\circ$, corresponding to the range of depth 0.962–0.938 $R_\odot$.

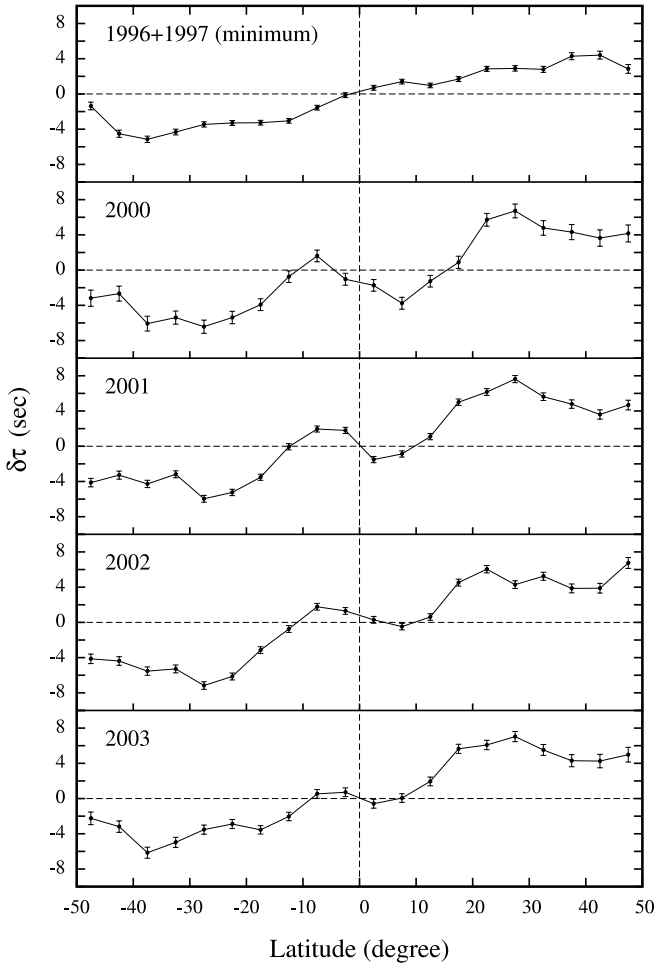


FIG. 3.—Time difference $\delta\tau$ vs. latitude for different years, showing the average over angular distance $10^\circ$–$16^\circ$, corresponding to the range of depth 0.938–0.901 $R_\odot$.

solar activity of Cycle 23 has double peaks in 2000 and 2001. The activity remains high until 2002. The sunspot number in 2003 drops to about half of its peak value at maximum, as shown in Figure 12.

Figures 1–5 show $\delta\tau$ versus latitude for five different distance ranges, corresponding to five different depth ranges. To see the evolution of meridional flows in the declining phase, each figure shows the yearly averaged $\delta\tau$ from 2000 to 2003. The average over the minimum period 1996–1997, $\delta\tau_{\rm min}$, is also included as the reference. The curve at minimum is smooth and has a sine-function shape for smaller $\Delta$. The error bar becomes greater, and the curve fluctuates more as it goes deeper, because the signal of the cross-correlation function becomes weaker. For larger $\Delta$, the curve is nearly linear across the equator and flattens at high latitudes.

The curves of 2000–2003 deviate from the curve of the minimum. The deviation is approximately antisymmetric with respect to the equator for all years at all depths. It is clear that the amplitude of the deviation decreased from 2000 to 2003 at all depths except $22^\circ$–$32^\circ$, which we discuss below. To see the change relative to minimum, $\delta\tau_{\rm min}$ is subtracted from $\delta\tau$ of each year; this is shown in Figures 6–10. The difference, $\delta\tau - \delta\tau_{\rm min}$, is approximately antisymmetric with respect to the equator. In each hemisphere, $\delta\tau - \delta\tau_{\rm min}$ is approximately antisymmetric with respect to latitude $\sim 15^\circ$–$20^\circ$. The above phenomena are consistent with the results in Paper I and Beck et al. (2002). The change in $\delta\tau$ has been interpreted as an additional divergent flow created in each hemisphere as activity developed. Figures 6–10 show that the amplitude of $\delta\tau - \delta\tau_{\rm min}$ decreased at all depths from 2000 to 2003 as the surface magnetic activity decreased. To see the evolution more clearly, we average $\delta\tau - \delta\tau_{\rm min}$ over $\Delta = 6^\circ$–$22^\circ$ to increase the S/N, because the amplitude of $\delta\tau - \delta\tau_{\rm min}$ in this distance range is greater. The averaged $\delta\tau - \delta\tau_{\rm min}$ over $\Delta = 6^\circ$–$22^\circ$ for different years is shown in Figure 11. It is clear that the amplitude of the divergent flow decreased from 2000 to 2003. To quantify the magnitude of the speed of the divergent flow, we average $|\delta\tau - \delta\tau_{\rm min}|$ over latitude ($-40^\circ$, $40^\circ$). The latitudinal average, $\langle|\delta\tau - \delta\tau_{\rm min}|\rangle$, for $\Delta = 6^\circ$–$16^\circ$ versus time is shown in Figure 12. The data of 1998 and 1999 are taken from Paper I. The sunspot number (Van der Linden et al. 2003) is also shown in Figure 12 for comparison. It is clearly shown in Figure 12 that the amplitude of the divergent flow correlates with the sunspot number.

Comparison of Figure 11 and the sunspot distribution indicates that the center of the additional divergent flow coincides with the center of the sunspot distribution, and it moves toward the equator with time. This phenomenon is consistent with the result of the rising phase of Cycle 23 (Paper I; Beck et al. 2002). The correlation of the amplitude and location of the divergent flow with surface activity suggests that the additional divergent flow has a magnetic origin.

The evolution of the additional divergent flow is not completely the same in the northern and southern hemispheres. For example, Figure 11 shows that the equatorward flow at low latitudes in the

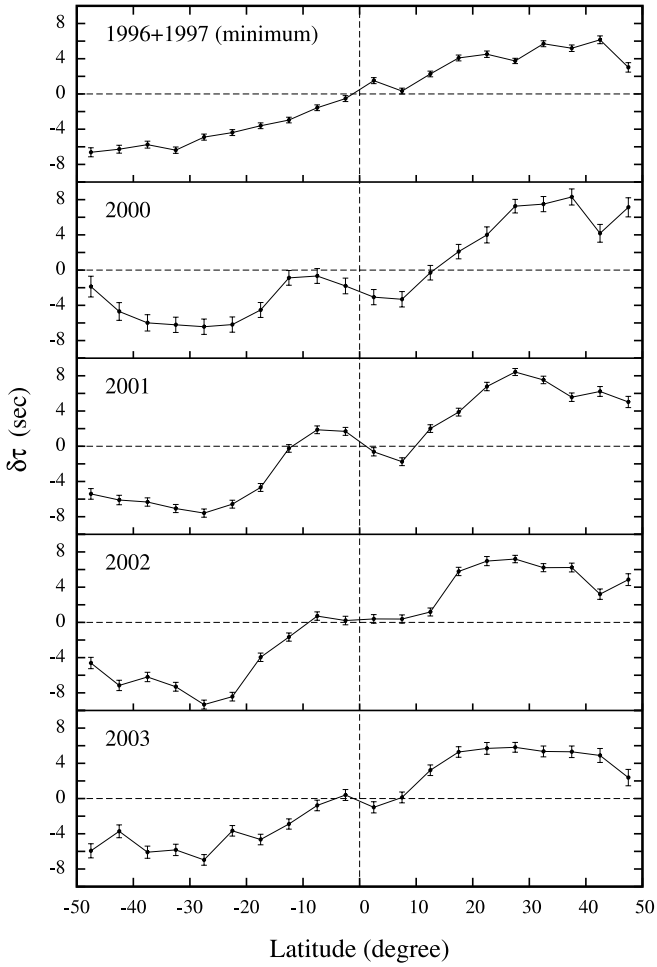


FIG. 4.—Time difference $\delta\tau$ vs. latitude for different years, showing the average over angular distance 16°–22°, corresponding to the range of depth 0.901–0.864 $R_\odot$.

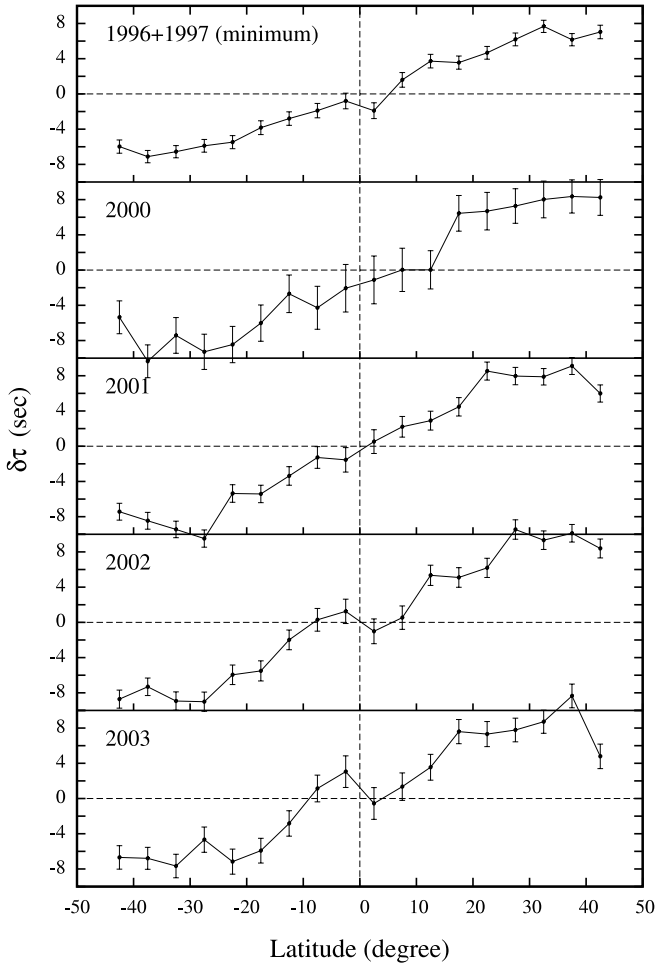


FIG. 5.—Time difference $\delta\tau$ vs. latitude for different years, showing the average over angular distance 22°–32°, corresponding to the range of depth 0.864–0.793 $R_\odot$.

northern hemisphere decreases more rapidly than at other latitudes. This might relate to the asymmetry of the sunspot numbers in the northern and southern hemispheres: the sunspot number in the northern hemisphere is greater than that in the southern hemisphere in the period 1999–2002 (Van der Linden et al. 2003).

## 4. DEPTH VARIATIONS OF MERIDIONAL FLOWS

Figures 6–10 show that the amplitude of the divergent flow changes with angular distance (or depth). To see its depth dependence more clearly, we average $\delta\tau - \delta\tau_{\min}$ over 2000–2002 to increase the S/N, because the activity is high in this period. The temporal-averaged $\delta\tau - \delta\tau_{\min}$ at different depths is shown in Figure 13. The amplitude of $\delta\tau - \delta\tau_{\min}$ increases with angular distance $\Delta$ and reaches its maximum at $\Delta = 10^\circ$–$16^\circ$, and declines slightly at $\Delta = 16^\circ$–$22^\circ$. The amplitude drops significantly at $\Delta = 22^\circ$–$32^\circ$. We could conclude from Figure 13 that the amplitude of $\delta\tau - \delta\tau_{\min}$ increases with depth from 0.987 $R_\odot$; it peaks at $\sim$0.9 $R_\odot$ and then decreases as it goes deeper. Although one needs to invert $\delta\tau$ to obtain the distribution of the divergent flow, the depth of the maximum amplitude of the divergent flow can be estimated with the $\Delta$-dependence of $\delta\tau - \delta\tau_{\min}$. Since $\delta\tau$ is proportional to the integral of the change in travel time along the ray path, the location of the maximum amplitude of the divergent flow is shallower than that of $\delta\tau - \delta\tau_{\min}$, which is about 0.9 $R_\odot$. Thus we conclude that the maximum amplitude of the divergent flow is located no deeper than 0.9 $R_\odot$.

It is of interest to note that the evolution of $\delta\tau$ for $\Delta = 22^\circ$–$32^\circ$, shown in Figures 5 and 10, is different from other angular distances. For $\Delta < 22^\circ$, the amplitude of $\delta\tau - \delta\tau_{\min}$ decreased from 2000 to 2003, as shown in Figures 6–9. For $\Delta = 22^\circ$–$32^\circ$, shown in Figure 5, the amplitude of the divergent flow is small. The shape of $\delta\tau$ for the minimum in 2000 and 2001 was more or less linear at low latitudes, but it began to deviate from the linear curve at low latitudes in 2002, and the deviation grew greater in 2003. This can also be seen in Figure 10, although the signal is less than 3 $\sigma$. It is not clear whether the changes in 2002 and 2003 at low latitudes are real signals. If they are real, the changes may correspond to the birth of a divergent flow at rather deep regions, 0.793–0.846 $R_\odot$, in the declining phase of Cycle 23. However, caution should be taken in interpreting $\delta\tau$ at low latitudes for large $\Delta$, because $\delta\tau$ includes the signals from another hemisphere. The $\delta\tau$ needs to be inverted to obtain the distribution of the meridional flow.

## 5. SUMMARY

A new divergent flow was created at active latitudes in both hemispheres as the surface activity developed. It extends from 0.987 $R_\odot$ at least down to 0.793 $R_\odot$. The amplitude of the divergent flow increases with depth until about 0.9 $R_\odot$, and then decreases with depth at least down to 0.793 $R_\odot$. The amplitude of the divergent flow correlates with the sunspot number. The center of the divergent flow coincides with the center of the sunspot

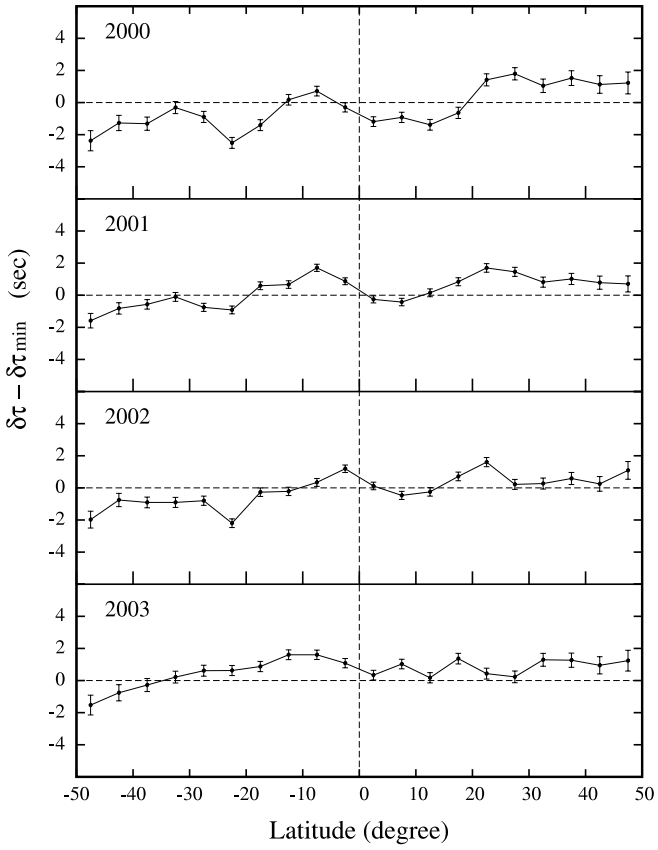


FIG. 6.—Time difference $\delta\tau$ relative to that of the minimum, $\delta\tau_{\rm min}$, for different years, showing the average over angular distance $2^\circ-6^\circ$, corresponding to the range of depth 0.987–0.962 $R_\odot$.

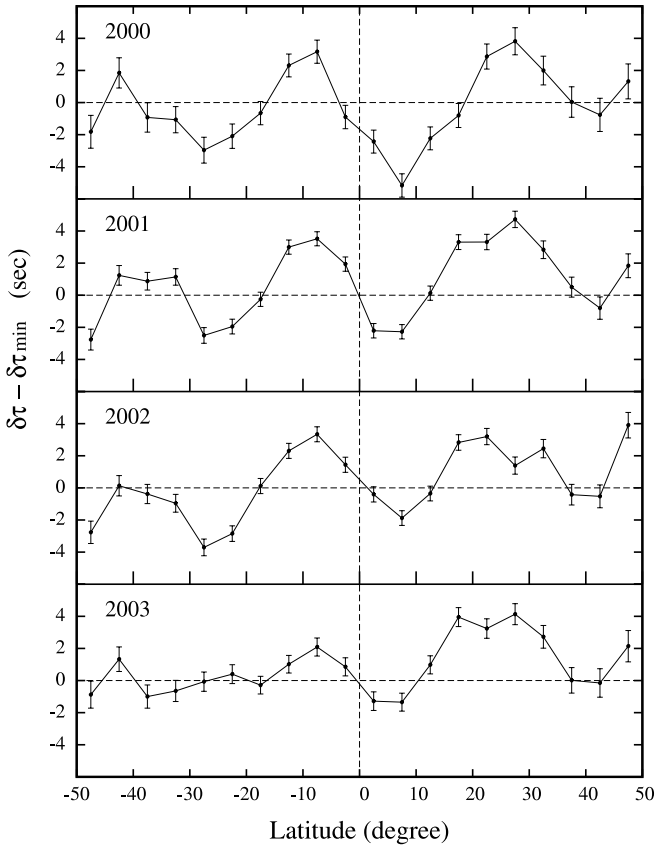


FIG. 8.—Time difference $\delta\tau$ relative to that of the minimum, $\delta\tau_{\rm min}$, for different years, showing the average over angular distance $10^\circ-16^\circ$, corresponding to the range of depth 0.938–0.901 $R_\odot$.

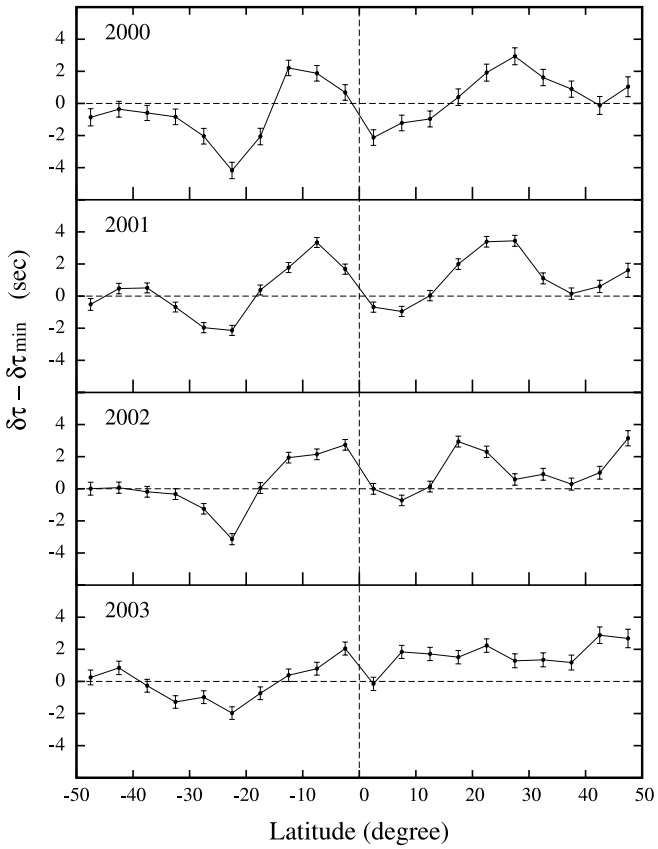


FIG. 7.—Time difference $\delta\tau$ relative to that of the minimum, $\delta\tau_{\rm min}$, for different years, showing the average over angular distance $6^\circ-10^\circ$, corresponding to the range of depth 0.962–0.938 $R_\odot$.

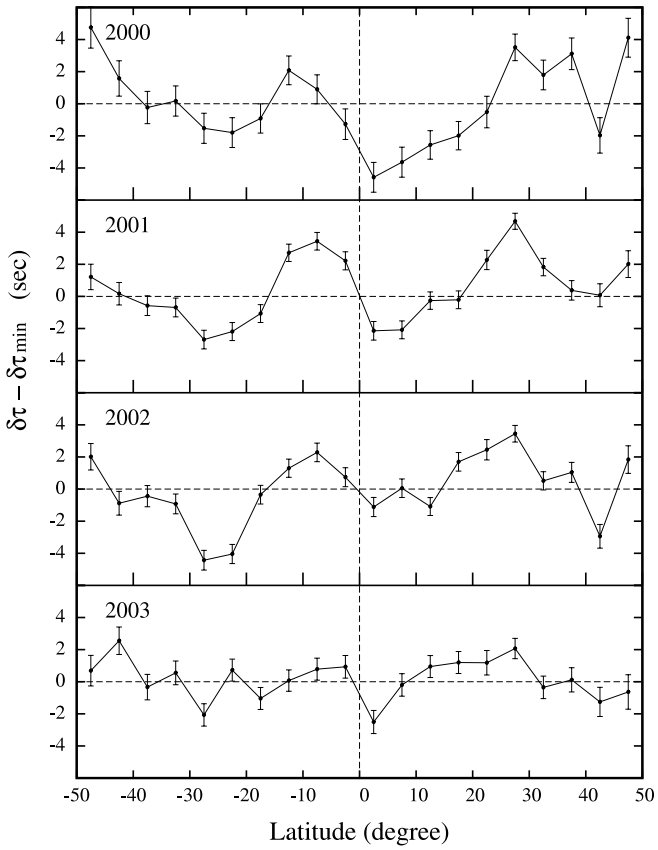


FIG. 9.—Time difference $\delta\tau$ relative to that of the minimum, $\delta\tau_{\rm min}$, for different years, showing the average over angular distance $16^\circ-22^\circ$, corresponding to the range of depth 0.901–0.864 $R_\odot$.

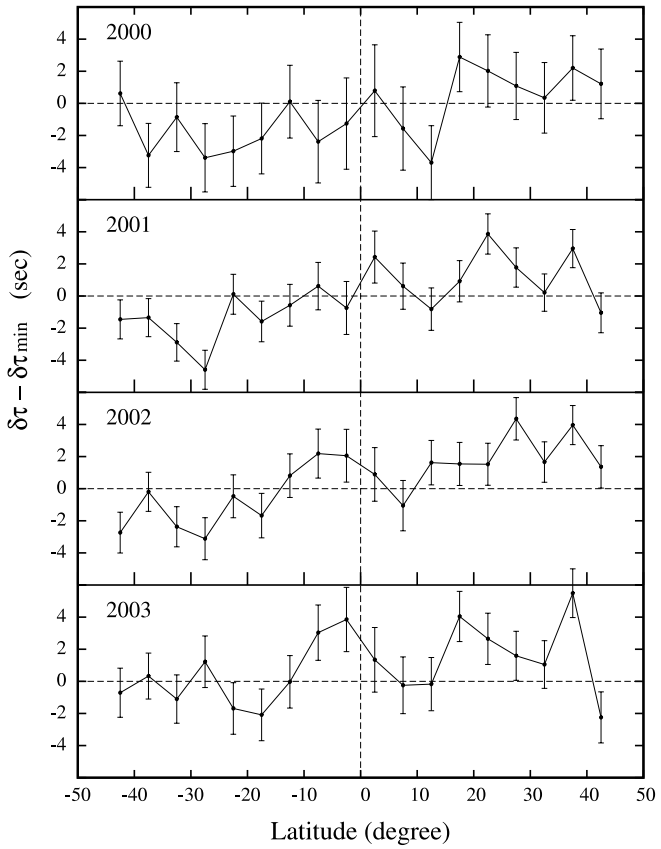


FIG. 10.—Time difference $\delta\tau$ relative to that of the minimum, $\delta\tau_{\rm min}$, for different years, showing the average over angular distance $22^\circ-32^\circ$, corresponding to the range of depth 0.864–0.793 $R_\odot$.

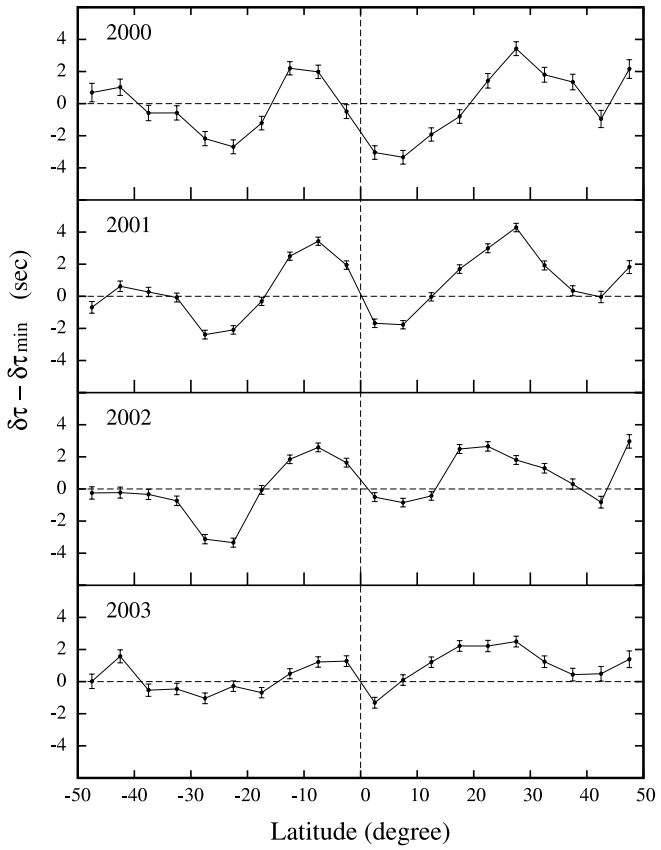


FIG. 11.—Plot of $\delta\tau - \delta\tau_{\rm min}$ averaged over angular distance $\Delta = 6^\circ-22^\circ$ for different years.

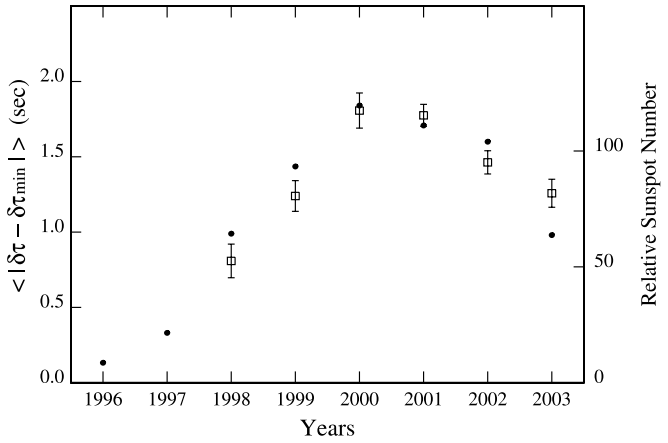


FIG. 12.—Plot of $|\delta\tau - \delta\tau_{\rm min}|$ averaged over latitude $(-40^\circ, 40^\circ)$ and angular distance $(\Delta = 6^\circ-16^\circ)$ vs. time. The data for 1998 and 1999 are taken from Paper I. The filled circles denote the relative sunspot number (Van der Linden et al. 2003).

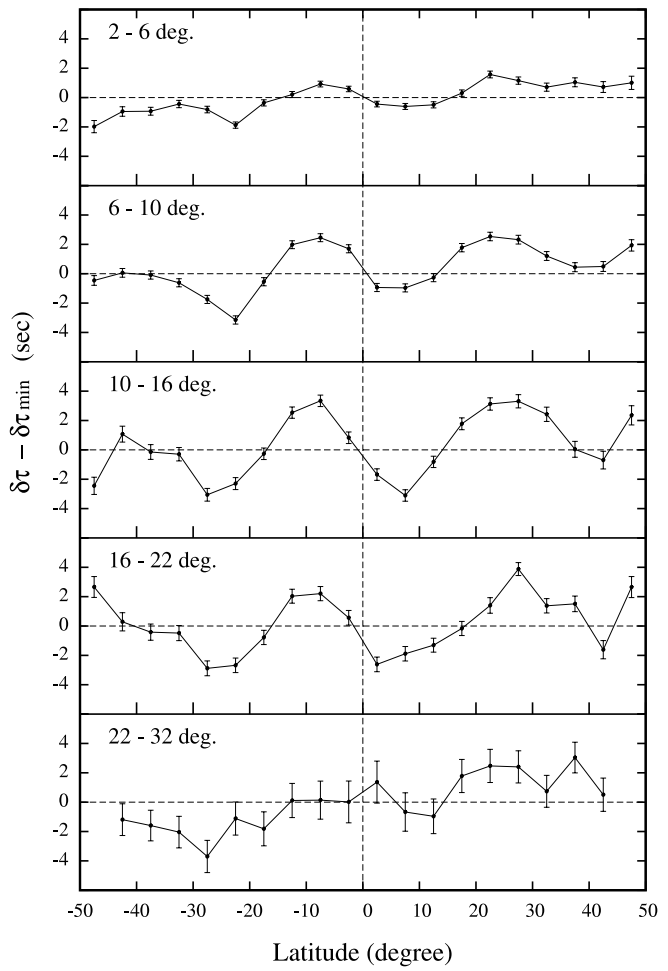


FIG. 13.—Time difference $\delta\tau$ averaged over 2000–2002, relative to that of the minimum, $\delta\tau_{\rm min}$ for different angular distances.

distribution. The correlation with the surface activity suggests that the divergent flow might have a magnetic origin. How the additional divergent flow is created and how it interacts with the rising magnetic flux tubes is unknown. The measurements in this study might provide some clues to this question.

We are grateful to the GONG Data Team for providing the software package GRASP. D.-Y. C. deeply thanks all members of the TON Team who were dedicated to the long-term observations. The TON Team includes Ming-Tsung Sun (Chang-Gung University, Taiwan), Antonio Jimenez (Instituto Astrofisica de Canarias, Spain), Guoxiang Ai and Honqi Zhang (Huairou Solar Observing Station, China), Philip Goode and William Marquette (Big Bear Solar Observatory, US), and Shuhrat Ehgamberdiev and Oleg Ladenkov (Ulugh Beg Astronomical Institute, Uzbekistan). Authors and the TON project were supported by the NSC of China, under grant NSC-93-2112-M-007-026.

REFERENCES

Basu, S., & Antia, H. M. 2000, Sol. Phys., 192, 469
Beck, J. G., Gizon, L., & Duvall, T. L., Jr. 2002, ApJ, 575, L47
Bracewell, R. N. 1986, The Fourier Transform and Its Applications (New York: McGraw-Hill).
Braun, D. C., & Fan, Y. 1998, ApJ, 508, L105
Chen, K.-R., et al. 1996, ApJ, 465, 985
Chou, D.-Y., & Dai, D.-C. 2001, ApJ, 559, L175 (Paper I)
Chou, D.-Y., et al. 1995, Sol. Phys., 160, 237
Duvall, T. L., Jr. 1979, Sol. Phys., 63, 3
Giles, P. M. 1999, Ph.D. thesis, Stanford Univ.
Giles, P. M., Duvall, T. L., Jr., & Scherrer, P. H. 1998, in Proc. SOHO 6/GONG 98 Workshop on Structure and Dynamics of the Interior of the Sun and Sun-like Stars, ed. S. Korzennik & A. Wilson (ESA SP-418; Noordwijk: ESA), 775
Giles, P. M., Duvall, T. L., Jr., Scherrer, P. H., & Bogart, R. S. 1997, Nature, 390, 52
Gonzalez Hernandez, L., et al. 1999, ApJ, 510, L153
Haber, D. A., Hindman, B. W., Toomre, J., Bogart, R. S., Larsen, R. M., & Hill, F. 2002, ApJ, 570, 855
Hathaway, D. H., et al. 1996, Science, 272, 1306
Howard, R. F., & Gilman, P. A. 1986, ApJ, 307, 389
Komm, R. W., Howard, R. F., & Harvey, J. W. 1993, Sol. Phys., 147, 207
LaBonte, B. J., & Howard, R. F. 1982, Sol. Phys., 80, 361
Meunier, N. 1999, ApJ, 527, 967
Nesme-Ribes, E., Meunier, N., & Vince, I. 1997, A&A, 321, 323
Snodgrass, H. B., & Dailey, S. B. 1996, Sol. Phys., 163, 21
Van der Linden, R. A. M., et al. 2003, Online Catalogue of the Sunspot Index (Brussels: Royal Observatory of Belgium), http://sidc.oma.be/html/sunspot.html